Resistance to an Irreversible Epidermal Growth Factor Receptor (EGFR) Inhibitor in EGFR-Mutant Lung Cancer Reveals Novel Treatment Strategies

Zhiwei Yu,[1,6] Titus J. Boggon,[3] Susumu Kobayashi,[4] Cheng Jin,[1] Patrick C. Ma,[1] Afshin Dowlati,[1] Jeffrey A. Kern,[2] Daniel G. Tenen,[5] and Balázs Halmos[1]

[1]Divisions of Hematology/Oncology and [2]Pulmonary, Critical Care and Sleep Medicine, Case Western Reserve University, Cleveland, Ohio; [3]Department of Pharmacology, Yale University School of Medicine, New Haven, Connecticut; [4]Beth Israel Deaconess Medical Center, Harvard Medical School; [5]Harvard Institutes of Medicine, Boston, Massachusetts; and [6]Harbin Medical University, Heilongjiang, China

Abstract

Patients with epidermal growth factor receptor (EGFR)–mutant non–small cell lung cancer derive significant clinical benefit from treatment with the EGFR tyrosine kinase inhibitors gefitinib and erlotinib. Secondary EGFR mutations such as EGFR T790M commonly lead to resistance to these agents, limiting their long-term efficacy. Irreversible EGFR inhibitors such as CL-387,785 can overcome resistance and are in clinical development, yet acquired resistance against these agents is anticipated. We carried out a cell-based, *in vitro* random mutagenesis screen to identify EGFR mutations that confer resistance to CL-387,785 using T790M-mutant H1975 lung adenocarcinoma cells. Mutations at several residues occurred repeatedly leading to functional resistance to CL-387,785. These variants showed uninhibited cell growth, reduced apoptosis, and persistent EGFR activation in the presence of CL-387,785 as compared with parental H1975 cells, thus confirming their role in resistance. A screen of alternative agents showed that both an alternative EGFR inhibitor and a cyclin-dependent kinase 4 inhibitor led to significant inhibition of cell growth of the resistant mutants, suggestive of potential alternative treatment strategies. These results identify novel mutations mediating resistance to irreversible EGFR inhibitors and reveal alternative strategies to overcome or prevent the development of resistance in EGFR-mutant non–small cell lung cancers. [Cancer Res 2007;67(21):10417–27]

Introduction

The epidermal growth factor receptor (EGFR) ATP-competitive tyrosine kinase inhibitors erlotinib and gefitinib showed success in the treatment of advanced non–small cell lung cancers following the failure of front-line chemotherapy (1). Approximately 10% to 25% of patients will have a major response to these agents, and erlotinib treatment leads to an overall survival advantage as compared with placebo in patients with chemorefractory non–small cell lung cancer (1). Most responding patients' tumors harbor recurrent somatic EGFR mutations (2–4). The most common of the EGFR mutations, L858R and exon 19 deletions affecting an LRE amino acid sequence, represent 85% to 90% of all mutations and are clear-cut predictors of major responses to this class of drugs (5–8). Whereas some responses are dramatic and durable, ultimately all patients seem to progress on continued EGFR tyrosine kinase inhibitor therapy. Secondary EGFR mutations, most commonly the EGFR T790M mutation, were identified as the mechanism of resistance to this class of agents (9–11). Resistance mediated by T790M can be overcome by irreversible EGFR inhibitors such as CL-387,785, HKI-272, and EKB-569 (11–13). Whereas such inhibitors are in clinical development and early signs of success have been reported in erlotinib-refractory lung cancers, it is clear that resistance develops against this class of inhibitors as well (14). We developed a cell-based random mutagenesis screen to identify resistance mechanisms to the model irreversible tyrosine kinase inhibitor CL-387,785 using T790M-mutant H1975 cells. Clinically relevant imatinib-resistant mutations of BCR-ABL and KIT almost exclusively occur in the exons encoding the tyrosine kinase domain (15, 16). Our current model system therefore focused on the kinase domain of EGFR to identify potentially clinically relevant resistance mutations. We also pursued further studies for the identification of alternative treatment strategies to overcome such resistance.

Materials and Methods

Cell culture and reagents. NIH-H1975 lung adenocarcinoma cells, which contain mutant EGFR-L858R-T790M (10), were propagated in RPMI 1640 supplemented with 10% fetal bovine serum (FBS) and 100 units/mL penicillin. All cells were grown at 37°C in a humidified atmosphere with 5% CO_2 and were in the logarithmic growth phase at the initiation of all experiments. CL-387,785, EGFR/ErbB2/ErbB4 inhibitor, cyclin-dependent kinase (Cdk)-4 inhibitor, LY294002, AG1478, and U0126 were purchased from Calbiochem (EMD Biosciences, Inc.). GW583340 was purchased from Sigma. Erlotinib was obtained from a commercial source. Drugs were dissolved in DMSO to give a 10 mmol/L stock solution and then stored at −20°C and the final DMSO concentration in all experiments was <0.1% in medium.

EGFR mutagenesis, library generation, and drug resistance screen. The plasmid construct pCDNA 3.1(−)-EGFR-L858R-T790M-HA was generated as previously described (9). This construct was further modified by mutating the GAGACG sequence to GTGACG through site-directed mutagenesis using the QuickChange mutagenesis kit (Stratagene), thereby destroying one of the two *Bsm*BI sites at position 1,011 (human EGFR, GeneBank ID NM005228) without changing the amino acid sequence. A 1,308-bp region of EGFR containing the entire tyrosine kinase domain of EGFR was amplified by PCR using the primers 5′-GAATGTCAGCCGA-GGCAGGGAATG-3′ (sense) and 5′-TCACGGAACTTTGGGCGACTATCT-3′ (antisense) in the presence of 50 μmol/L $MnCl_2$, which reduces the fidelity

of Taq and thereby promotes the introduction of errors leading to random point mutations (17). Subcloning into p-GEM-T Easy vector and sequencing of individual colonies showed that essentially all of the PCR products contained mutations, with 50% of the products containing a 1-bp change, showing the success of the mutagenesis procedure. The pool of amplified DNA fragments was digested with *Bsm*BI and *Cla*I, gel purified after dephosphorylation with calf intestinal phosphatase at 37°C for 1 h to avoid self-ligation, and religated into the backbone pCDNA 3.1(−)-EGFR-L858R-T790M-HA vector. Parental NIH-H1975 cells were transfected with the mutagenized libraries by the use of Fugene 6 reagent (Roche). Culture supernatants were replaced by fresh medium containing 500 μg/mL neomycin and 1 μmol/L CL-387,785 after 24 h. Culture medium was changed every 2 to 3 days with addition of G418 and fresh CL-387,785. Nearly 1 month later, isolated cell colonies that became visible were picked and amplified in liquid culture in the presence of both neomycin and CL-387,785.

Genomic DNA from the neomycin and CL-387,785–resistant cells was isolated. Relevant regions of the transfected EGFR DNA were recovered by PCR amplification with the use of primers 5′-GGTCTGCCATGCCT-TGTGCTC-3′ (sense) and 5′-ATCCATCAGGGCACGGTAGAAGTT-3′ (anti-sense) and the PCR products were sequenced to identify the mutations that may lead to drug resistance. For sequencing, the following primers were used: primer set 1, 5′-GGTCTGCCATGCCTTGTGCTC-3′ (sense) and 5′-GTGCGCTTCCGAACGATGTA-3′ (antisense); primer set 2, 5′-GATGGT-GGGGGCCCTCCTCTT-3′ (sense) and 5′-CTTTCTCTTCCGCACCCAGCAG-TT-3′ (antisense); and primer set 3, 5′-TCCGGGAACACAAAGACAATA-3′ (sense) 5′-ATCCATCAGGGCACGGTAGAAGTT-3′ (antisense). Of note is that the obtained sequences were plasmid derived because the sequenc-

ing primers spanned several exons; therefore, genomic EGFR would not be expected to be amplified with the use of these primers. Sequence alignment and analysis was done with DNASTAR and Mutation SURVEYOR software (SoftGenetics).

Generation of EGFR mutants. Four of the mutations identified repeatedly in the isolated clones were regenerated by site-directed mutagenesis (QuickChange) of the previously listed pCDNA3.1(−)-EGFR-L858R-T790M-HA plasmid construct. The site of mutations and primers used for site-directed mutagenesis were L655H, 5′-GGGGGCCCTCCACTT-GCTGCTGG-3′ (sense) and 5′-CCAGCAGCAAGTGGAGGGCCCCC-3′ (anti-sense); L658P, 5′-CCTCCTCTTGCTGCCGGTGGTGGCCCTGG-3′ (sense) and 5′-CCAGGGCCACCACCGGCAGCAAGAGGAGG-3′ (antisense); H773L, 5′-GGACAACCCCCTCGTGTG-3′ (sense) and 5′-CACACGAGGGGGTTGT-CC-3′ (antisense); and E931G, 5′-CCATCCTGGAGAAAGGAGGACGCCTC-CCTCAGC-3′ (sense) and 5′-GCTGAGGGAGGCGTCCTCCTTTCTCCAGGA-TGG-3′ (antisense). Two of these mutations, E931G and L658P, were similarly reengineered into the pCDNA3.1(−)-EGFR-L858R-HA plasmid (non-T790M). The proper sequence of all generated constructs was confirmed by resequencing. Transient transfection studies were done using Cos-7 cells with these reconstructed plasmids. Western blot analyses were used to confirm the success of transfection with the use of an anti-hemagglutinin tag antibody.

The irreversible inhibitor CL-387,785 blocks the EGFR kinase enzymatic function by covalently binding to Cys[797] of EGFR (18–21). We generated the C797S mutation in our pCDNA3.1(−)-EGFR-L858R-T790M-HA construct by site-directed mutagenesis using primers 5′-GCTCATGCCCTTCG-GCTCCCTCCTGGACTATGTCCG-3′ (sense) and 5′-CGGACATAGTCCAGG-AGGGAGCCGAAGGGCATGAGC-3′ (antisense), and then transfected it onto
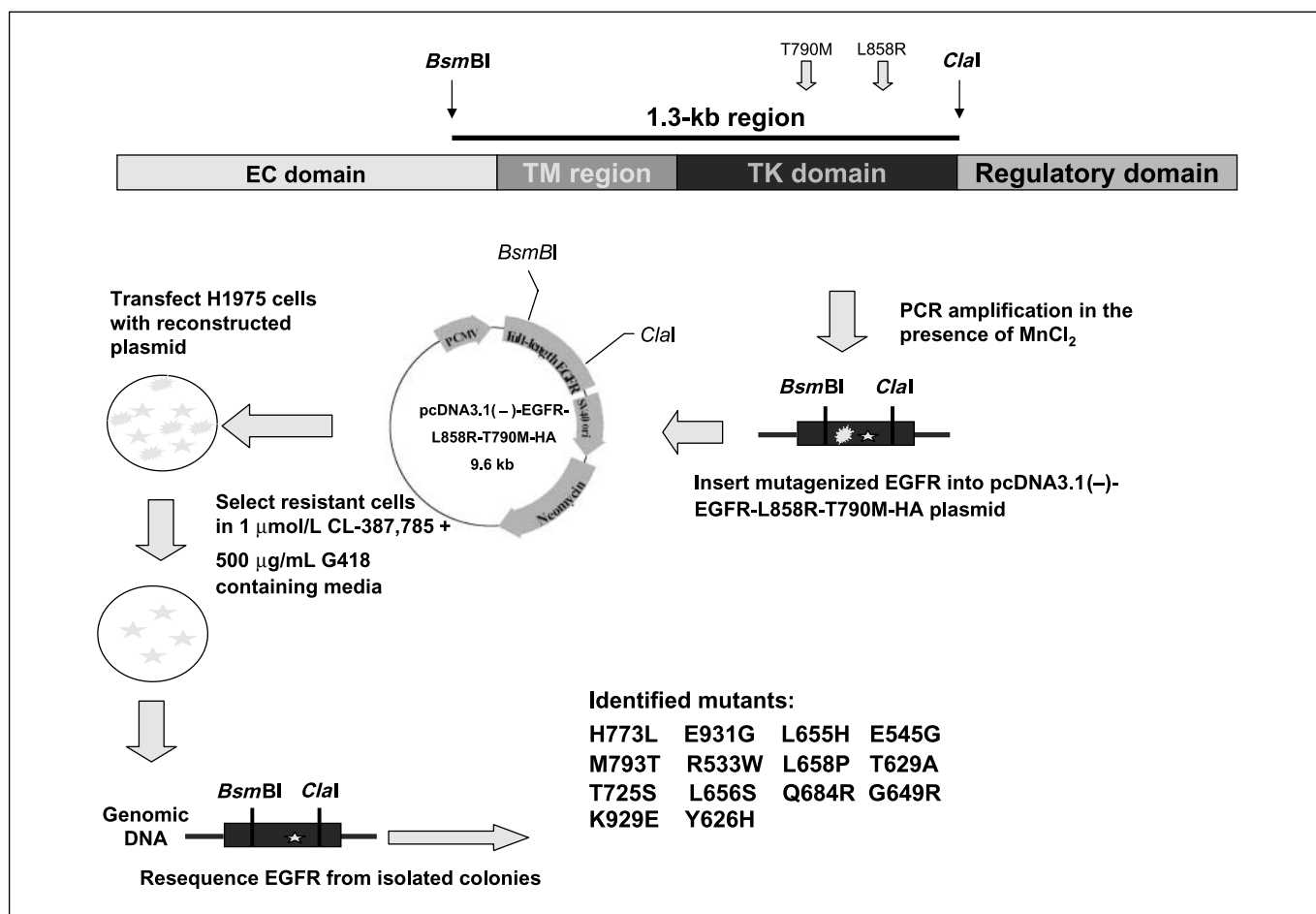

Figure 1. Strategy for the random mutagenesis of EGFR and steps followed to identify the mutations that confer resistance to CL-387,785.

Table 1. Point mutants recovered in 1 μmol/L CL-387,785

Mutation	No. mutants (%)	IC$_{50}$ (μmol/L)	Fold parental IC$_{50}$
E931G	8 (27.6)	2.65	7.4
L658P	4 (13.8)	3.76	10.5
L655H	3 (10.3)	1.95	5.4
H773L	2 (6.9)	6.69	18.6
Q684R	2 (6.9)	ND	
E545G	2 (6.9)	ND	
M793T	1 (3.4)	ND	
R533W	1 (3.4)	ND	
T629A	1 (3.4)	ND	
T725S	1 (3.4)	ND	
L656S	1 (3.4)	ND	
G649R	1 (3.4)	ND	
K929E	1 (3.4)	ND	
Y626H	1 (3.4)	ND	
C797S	0	1.12	3.1
Non-mutations	12		

NOTE: IC$_{50}$ for H1975 is 0.36 μmol/L CL-387,785. Altogether, 34 resistant clones were examined and sequenced.

Abbreviation: ND, not determined.

NIH-H1975 cells. G418 (500 μg/mL) was used to select stably transfected cells and isolated colonies were picked using cloning rings and continued to be cultured in the presence of G418. Sequencing was done to confirm the presence of the mutant C797S DNA in the cells with the primers as listed earlier. Expression of the EGFR-C797S mutant was confirmed by the detection of the expression of the hemagglutinin tag as above.

Protein immunoblotting. Cells were serum starved overnight and then incubated with various concentrations of different EGFR inhibitors for 3 h or Cdk4 inhibitor for 24 h before EGF (100 ng/mL; Sigma) stimulation (37°C, 15 min). After treatment, cells were lysed with 10% TCA lysis buffer and lysates were clarified by centrifugation. Proteins were separated by 7.5% SDS-PAGE gel and transferred onto nitrocellulose membranes (Bio-Rad) for Western blot analysis. Antibodies to EGFR (SC-3), anti-EGFR-phycoerythrin, and hemagglutinin tag were purchased from Santa Cruz Biotechnology. Antibodies directed against phosphorylated EGFR (pY1068), total extracellular signal–regulated kinase (ERK) and phosphorylated ERK, and total Akt and phosphorylated Akt, and Rb (Ser[780], Ser[795], Ser[807/811]) Antibody Kit were purchased from Cell Signaling. The β-actin antibody was purchased from Sigma-Aldrich. After washing and incubation with secondary antibodies, blots were developed with a chemiluminescence system (Perkin-Elmer).

Cell viability assay to determine IC$_{50}$. NIH-1975 cells (6×10^3) and its subclones expressing tyrosine kinase inhibitor–resistant mutant EGFR proteins were plated in each well of 96-well plates in RPMI 1640 containing 10% FBS. The following day, dilutions of compound were added to the media in increasing concentrations (final concentration: 0, 0.2, 0.6, 2.0, 6.0, and 20 μmol/L). The concentration of DMSO in the medium was adjusted to 0.1%. After 72 h of incubation, viable cell numbers were measured by using 3-(4,5-dimethylthiazol-2-yl)-5-(3-carboxymethoxyphenyl)-2-(4-sulfophenyl)-2*H*-tetrazolium, inner salt (MTS; absorption of formazan at 490 nm; CellTiter96, Promega) according to the manufacturer's protocol. Each assay consisted of six replicate wells of the same drug concentration. The IC$_{50}$ was determined from the dose-response curve.

Apoptosis analysis. Parental NIH-H1975 cells and CL-387,785–resistant H1975 clones were plated at a density of 3×10^5 per well in six-well plates. Twenty-four hours after plating, cell culture medium was replaced by fresh medium containing 10% FBS with or without 1 or 2 μmol/L of CL-387,785 or EGFR/ErbB2/ErbB4 inhibitor, and incubated for another 48 h. Apoptosis was assessed with the Annexin V-FLUOS staining kit (Roche) according to the instructions of the manufacturer.

Cell cycle analysis. Cells were incubated with Cdk4 inhibitor (0–6 μmol/L) in six-well plates for 24 and 72 h before collection. Cells were pulse labeled for 45 min with 10 μmol/L bromodeoxyuridine (BrdUrd; BD PharMingen, BD Biosciences), collected by trypsinization, washed, fixed, and stained with anti-bromodeoxyuridine-FITC conjugates (BD Biosciences), then counterstained with 7-amino-actinomycin D and analyzed by flow cytometry (FACSort; BD Biosciences). Data were analyzed using WINMDI software.

Structural analysis. The crystal structures of the kinase domain were downloaded from the Protein Data Bank (accession codes 1M14, 1M17, 1XKK, 2GS2, 2GS6, and 2GS7; refs. 22–24) and the structures analyzed using the program O (25).

Results

Random mutagenesis strategy for the identification of EGFR mutations conferring resistance to CL-387,785. To generate a library of point mutants of the EGFR tyrosine kinase binding domain, we randomly mutagenized a pCDNA 3.1(−)-EGFR-L858R-T790M-HA plasmid construct using PCR conditions of reduced Taq polymerase fidelity (Fig. 1). Following digestion with *Bsm*BI and *Cla*I, we religated a 1,308-bp region spanning the entire tyrosine kinase domain of the mutated plasmid pool back into the original plasmid backbone. Parental H1975 cells were then transfected with this plasmid pool and subsequently selected for colony growth in the presence of both 500 μg/mL G418 and 1 μmol/L CL-387,785 to identify transformation-competent and drug-resistant variants. H1975 cells carry double-mutant EGFR-L858R-T790M (10) and were previously shown to be resistant to gefitinib or erlotinib (IC$_{50}$ >10 μmol/L) but sensitive to CL-387,785 (IC$_{50}$, 0.36 μmol/L; ref. 12). Because growth curves and MTS assays showed that at 1 μmol/L CL-387,785 there is complete and sustained proliferation arrest of H1975 cells (Supplementary Fig. S1), this concentration was used for these studies. Thirty days after transfection, well-separated individual colonies were plucked with the use of cloning rings and 31 clones were successfully expanded. Limiting dilution was used as a second selection strategy and three colonies identified through this selection were further expanded.
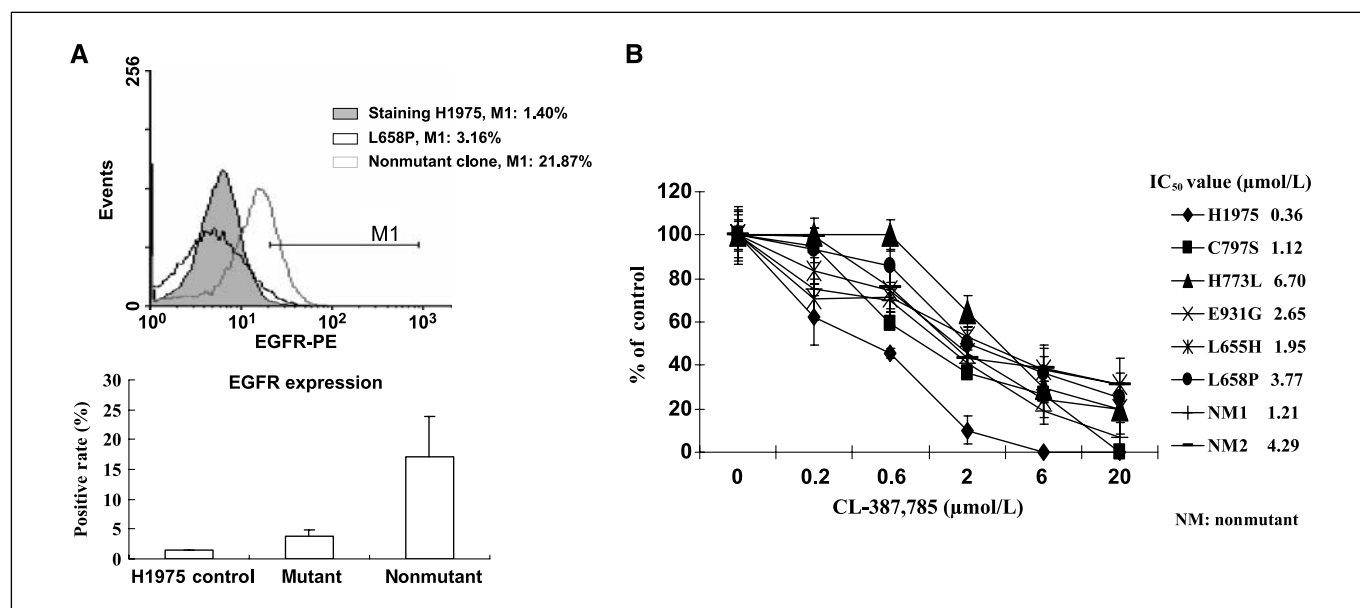
Figure 2. Biochemical and cellular assays of mutant sensitivity. *A,* EGFR expression in H1975, four nonmutant clones, and five mutant clones (L658P, E931G, L655H, H773L, and L656S) detected by flow cytometry through staining with EGFR-phycoerythrin (*PE*) antibody. The overlay histogram shows representative histograms of control H1975, L658P, and a nonmutant clone. *B,* dose-dependent growth inhibition of H1975 cells expressing different mutant and nonmutant clones as detected by the MTS assay.

From the expanded colonies, genomic DNA was isolated and the entire mutated kinase domain region of the *EGFR* gene was amplified by PCR. The resultant PCR products were bidirectionally sequenced to identify mutations. Sequence analysis revealed several previously undescribed point mutations. From 34 drug-resistant colonies (31 from the first and 3 from the second selection strategy), we identified 29 distinct amino acid substitutions affecting 14 residues (Table 1). Substitutions at six positions were identified more than once: E931G (8 cases), L658P (4 cases), L655H (3 cases), H773L (2 cases), Q684R (2 cases), and E545G (2 cases). From the first selection strategy, 12 colonies contained only wild-type EGFR sequences (one of these had a silent basepair change at K713), 13 clones contained a single EGFR mutation, and 6 clones contained double mutations (E545G/M793T, R533W/L658P, E931G/H773L, G649R/K929E, and E931G/Q684R twice). All of the three resistant clones identified through our limiting dilution strategy contained sequence alterations: one clone contained two mutations, T629A and T725S, and a silent basepair change at position I891, whereas the other two contained a single mutation each (clone 2, L655H; clone 3, L656S). Interestingly, the L655H mutation was identified in both selection strategies. The fact that several mutations were repeatedly identified strongly suggested a functional role for the identified mutations.

Characterization of the identified EGFR mutants. To preclude that drug resistance could be mediated by altered expression of EGFR, we examined cell-surface EGFR expression by flow cytometry in multiple identified colonies including five with detected mutations (L658P, E931G, L655H, H773L, and L656S) as well as four without detectable mutations. There was no difference in EGFR expression between parental H1975 cells and mutant H1975 colonies, whereas significantly higher expression of EGFR was noted in all nonmutant, drug-resistant colonies examined (Fig. 2*A*). This suggests that in these nonmutant colonies, resistance to CL-387,785 might be mediated by higher overall expression of EGFR.

To verify the functional relevance of the isolated EGFR variants, we studied H1975 clones stably expressing four of the frequently encountered mutations (E931G, H773L, L658P, and L655H). We also generated stably transfected H1975 cell lines expressing pCDNA3.1(−)-EGFR-L858R-T790M-C797S-HA plasmid constructs to model resistance as a result of this hypothesized resistance mutation that abrogates covalent binding of irreversible EGFR inhibitors such as CL-387,785 (18, 21). We confirmed equivalent expression of the transfected EGFR protein by detecting uniform expression of the hemagglutinin tag in these stable cell lines (Fig. 2*C*). We assessed the level of resistance that each of the identified mutations conferred to CL-387,785 by generating dose-response curves of each cell line by MTS assays. Cells were cultured in the presence of increasing concentrations of CL-387,785 ranging from 0 to 20 μmol/L. Parental H1975 cells were potently inhibited by CL-387,785 (IC$_{50}$, 0.36 μmol/L) as previously reported (12). H1975 cells expressing mutant EGFR forms were less sensitive to CL-387,785 with IC$_{50}$s ranging from 1.12 to 6.70 μmol/L. Two of the nonmutant clones were also examined and were similarly found to have increased IC$_{50}$s of 1.21 and 4.29 μmol/L, respectively (Fig. 2*B*).

Immunoblot analyses on protein lysates of H1975 cells incubated with increasing doses of CL-387,785 were also done to examine the effect of the drug on the phosphorylation of EGFR and its main downstream signaling effectors, AKT and ERK. In parental H1975 cells, 1 μmol/L CL-387,785 completely inhibited phosphorylation of EGFR and all of its examined downstream signaling effectors (Fig. 2*C*). In contrast, all the variants showed persistent EGFR phosphorylation in the presence of CL-387,785 at concentrations ranging from 1 to 3 μmol/L, confirming an ~3- to 10-fold shift in drug sensitivity corresponding to the findings of the MTS assays. Similarly, both ERK and AKT phosphorylation persisted at higher drug concentrations than in parental H1975 cells whereas total levels of EGFR, ERK, and AKT remained unchanged.

Next, all four mutations (E931G, H773L, L658P, and L655H) were regenerated by site-directed mutagenesis and used for transient
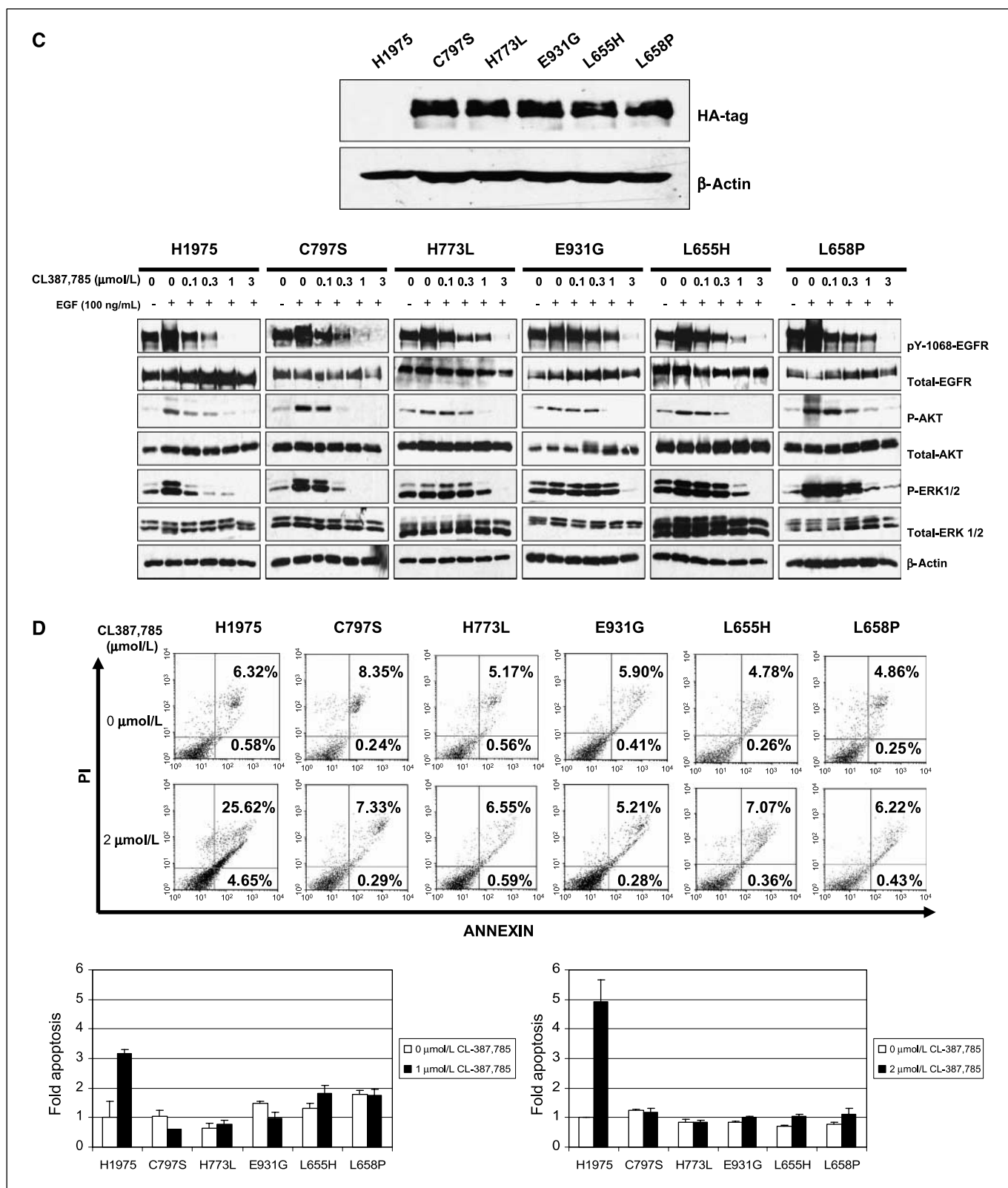
Figure 2 *Continued. C,* Western blotting shows equal expression of transfected EGFR as detected by expression of hemagglutinin (*HA*) tag by the use of an anti-hemagglutinin antibody. β-Actin serves as control. Dose response of CL-387,785 on phosphorylation of EGFR, AKT, and mitogen-activated protein kinase in parental H1975 and EGFR-mutant cells. Cells were treated with CL-387,785 at indicated concentrations for 3 h before treatment with 100 ng/mL EGF. Western blots are shown for phospho- and total EGFR, AKT, and ERK. β-Actin serves as control. *D,* CL-387,785 induces apoptosis in H1975 but not in mutant H1975 cells. *Top,* representative Annexin V/propidium iodide flow cytometry histograms; the numbers represent percent cells in the appropriate quadrant. *Left bottom quadrant,* viable cells; *right bottom quadrant,* early apoptotic cells; *right top quadrant,* late apoptotic cells. *Bottom, columns,* fold changes in apoptosis; *bars,* SD. H1975 and stably mutant H1975 were grown in the absence or presence of 1 or 2 μmol/L of CL-387,785 for 48 h.
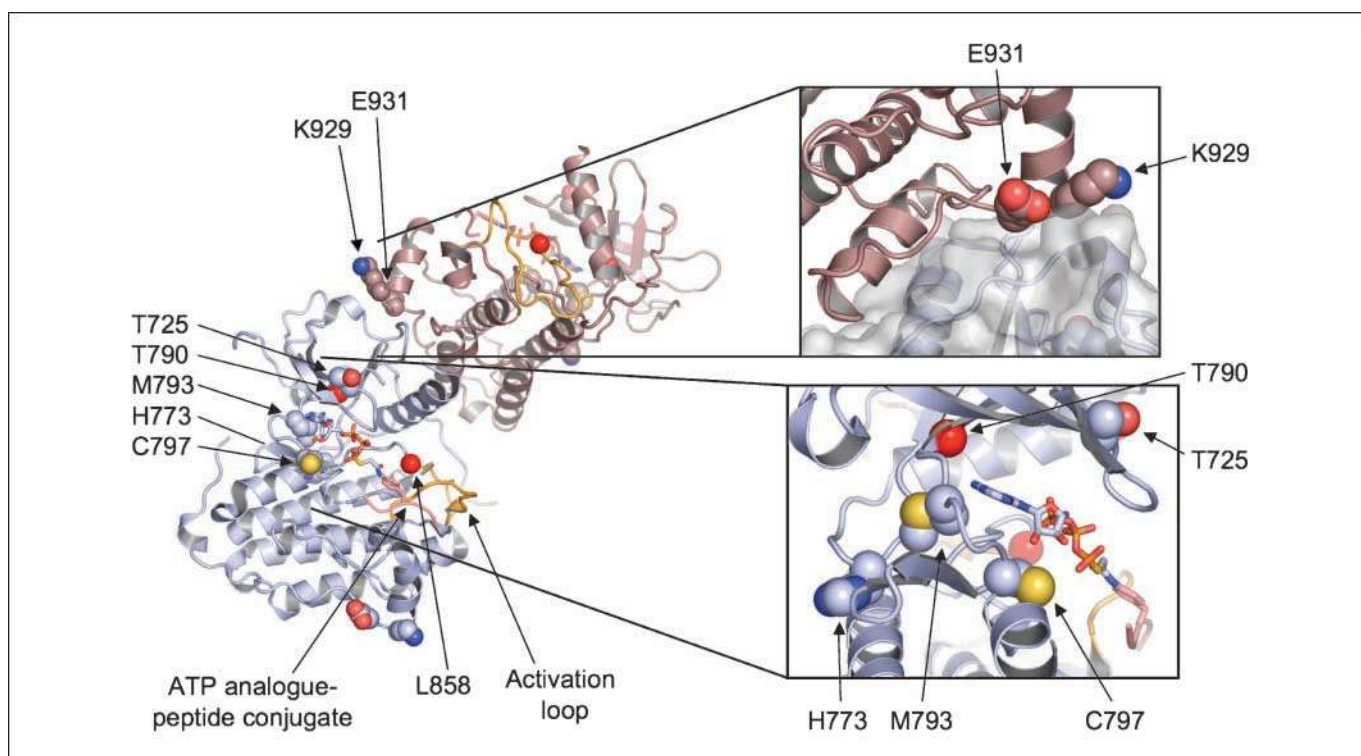
Figure 3. Structural analysis of the EGFR kinase domain mutations. The EGFR kinase domain crystal structure (PDB accession code 2GS6) is shown in complex with an ATP analogue-peptide conjugate. Two kinase domains are depicted here to illustrate the Cdk/cyclin-like activating asymmetrical dimerization interface elegantly proposed by Zhang et al. (24). The two EGFR kinase domain molecules are shown in cartoon format and colored blue and brown with their activation loops colored orange. The kinase domain mutations identified in this study are indicated with space-filling spheres and are colored with oxygen atoms in red and nitrogen atoms in blue. The locations of activating mutation L858R and the resistance mutation T790M are indicated with red spheres. The ATP analogue-peptide conjugate solved in this crystal structure is indicated with the ATP moiety shown in stick format and colored according to atom type. The top exploded view shows the location of residues E931 and K929 in the intermolecular interface packed against the surface (in *gray*) of the partner kinase domain. The bottom exploded view shows the location of the mutations found in the vicinity of the ATP-binding pocket. The figure was prepared using the program PYMOL (http://www.pymol.org).

transfection studies in Cos-7 cells. Expression of the mutant EGFRs was confirmed by detection of the hemagglutinin-tagged EGFR. Immunoblotting studies to detect phospho- and total EGFR, AKT, and ERK expression levels were then done with varying concentrations of CL-387,785 in the presence of EGF stimulation. These transfection studies confirmed resistance to CL-387,785 similar to the findings in H1975 stable transfectants (Supplementary Fig. S2). We further analyzed the functional consequences of these mutations by assessing cellular apoptosis induced by CL-387,785 as defined by Annexin V/propidium iodide apoptosis assays. Treatment of NIH-H1975 cells with 1 and 2 µmol/L of CL-387,785 resulted in a concentration-dependent prominent increase in the percentage of apoptotic cells, whereas the same concentrations had essentially no effect on apoptosis in any of the five mutant H1975 cell clones examined (Fig. 2*D*).

Next, we regenerated two of these mutant forms, E931G and L658P, in a EGFR-L858R-HA background to test whether these mutations confer resistance to reversible inhibitors such as erlotinib. Transient transfection studies of Cos-7 cells with these constructs showed an ~3-fold shift of the IC_{50} of these two mutant forms versus the parental plasmid, suggestive of functional resistance against reversible EGFR tyrosine kinase inhibitors such as erlotinib (Supplementary Fig. S3).

Structural analysis of the identified EGFR mutations. There are now multiple published EGFR kinase domain crystal structures (22–24, 26, 27). We mapped the three-dimensional locations of the residues affected by the point mutations onto these solved crystal

structures of the EGFR tyrosine kinase domain (Fig. 3). Of the four mutations that were further tested in this study, E931G, L658P, L655H, and H773L, two occur in the kinase domain. Mutation E931G occurs in a residue proximal to the proposed dimerization activation interface (24). In the EGFR crystal structures, E931 can form an intermolecular salt bridge with K708; however, E931 is not completely buried in the dimerization interface. Residue H773 is located in the loop between helix αC and strand β4. This residue forms a hydrogen bond to the backbone carbonyl oxygen of V851 and is above 10 Å distal from the kinase catalytic cleft. Both the L655H and L658P mutations occur outside of the solved EGFR kinase domain crystal structures; however, sequence analysis suggests that these residues are located in a conserved stretch of leucines that is part of the receptor single-pass transmembrane helix. For the mutations that were not further tested in this study, four occur in domain IV of the extracellular region (R533W, E545G, Y626H, and T629A), two occur in the transmembrane helix (G649R and L656S), and one occurs in the juxtamembrane region (Q684R). The remaining mutations are located in the kinase domain, two in close proximity to the adenosine pocket of the catalytic cleft (T725S and M793T) and one adjacent to the frequently seen E931G mutation (K929E).

An alternative EGFR inhibitor can overcome resistance. Next, we tested the above examined five CL-387,785–resistant H1975 clones against a panel of EGFR inhibitors including AG1478 (reversible EGFR inhibitor), GW583340 (reversible EGFR/ErbB2 inhibitor), and an irreversible EGFR/ErbB2/ErbB4 inhibitor (Calbiochem).

We carried out standard MTS assays following 72 h of drug treatment using a range of concentrations from 0 to 20 μmol/L. Whereas all mutant clones showed high-level resistance to AG1478 and GW583340 (data not shown), the EGFR/ErbB2/ErbB4 inhibitor (chemical structure shown in Supplementary Fig. S4) showed varying degrees of maintained efficacy against all the mutant clones tested (Fig. 4A). As compared with parental H1975 cells, this inhibitor was as effective against L655H and only slightly less effective against C797S and H773L mutant cells. Whereas a higher level of resistance was noted against L658P and E931G cells, the drug concentrations required to overcome resistance still suggest potential clinical relevance. Signaling studies also showed that treatment with the EGFR/ErbB2/ErbB4 inhibitor can potently inhibit EGFR Y-1068 phosphorylation as well as downstream signaling correlates such as phospho-AKT and ERK (Fig. 4B). Annexin/ propidium iodide studies further showed the induction of apoptosis by this compound in both parental H1975 cells and all five clones (E931G, L665H, L658P, H773L, and C797S) examined (Fig. 4C and D).

Downstream signaling inhibition identifies the use of Cdk4 inhibitors as a potential treatment strategy. We further sought to determine whether inhibition of downstream signaling pathways might also be a potentially effective treatment strategy. We were particularly interested in studying the effect of inhibition of the cyclin D/Cdk4 axis because our prior studies showed the functional significance of this pathway in oncogenic EGFR signaling (28). Therefore, we focused our studies on the potential efficacy of Cdk4 inhibition. The Cdk4 inhibitor used in these studies showed uniform activity against both parental H1975 cells and all five mutant clones tested in BrdUrd proliferation studies. Consistent with the effects on retinoblastoma (Rb) dephosphorylation, the Cdk4 inhibitor drug blocked cell cycle progression, resulting in a sharp decrease in the number of cells in the S phase of the cell cycle at a concentration of 2 μmol/L (Fig. 5A and B). An increased number of cells in the sub-G_1 fraction at 72 h of drug treatment was also observed in all clones examined, consistent with the induction of apoptosis (Fig. 5A and B). Immunoblotting showed that Cdk4 inhibitor treatment resulted in dephosphorylation of Rb protein at Ser^{780}, Ser^{795}, and $Ser^{807/811}$ in all mutants, consistent with inhibition of cyclin D/Cdk4 (Fig. 5C). Dephosphorylation occurred at drug concentrations (0.6–2 μmol/L) where the induction of growth arrest was also observed. These results suggest that blockade of the cyclin D/Cdk4 axis could be a potential alternative target in EGFR-mutant cells.

Discussion

In our current study, we show the functional relevance of secondary EGFR mutations as potential resistance mechanisms against irreversible EGFR inhibitors, modeled by CL-387,785, in EGFR-mutant non–small cell lung cancer. Our cell-based random mutagenesis approach identified numerous secondary mutations of EGFR. Several of these mutations were repeatedly identified, strongly suggestive of their functional relevance. Four of these mutants were chosen for further studies, and all four were confirmed to lead to functional resistance to CL-387,785. The IC_{50} of these mutants ranged from 1.1 to 6.7 μmol/L (3–19-fold resistance over parental cells). Because many imatinib-resistant mutations of BCR-ABL as well as the recently identified D761Y mutation of EGFR lead to an IC_{50} shift in this range, we predict that these mutations will be clinically relevant (15, 29, 30).

The mutations described in our study broadly fall into four categories: kinase domain mutations close to the activating interface, mutations in the kinase domain close to the adenosine binding region of the catalytic cleft, mutations within the transmembrane helix, and extracellular mutations. Approximately half of the mutations that we discovered were in the kinase domain of EGFR and were dominated by E931G. This mutation was recovered in eight independent clones and the nearby mutation K929E occurred in one further clone. Both E931 and K929 are conserved residues located on the periphery of the proposed kinase-activating asymmetrical dimer interface in the kinase domain crystal structures. Indeed, in the study of Zhang et al. (24), both K929 and E931 were predicted to be important in the activation of the cyclin/Cdk-like asymmetrical EGFR dimer, suggesting that these mutations could potentially affect the dimerization and activation potential of EGFR. It is interesting to note that the double mutation E931G + Q684R arose twice in this study; the mutation Q684R is in the EGFR juxtamembrane region. This may suggest a role in regulation and resistance for an interaction between the juxtamembrane region and the C-lobe of the EGFR kinase domain. Our structural analysis also suggested that many of the mutations may have an effect on the kinase catalytic cleft. Mutation H773L occurs at a residue position dominated by histidine and asparagine residues in human kinases. These residues are able to form hydrogen bonds; in the EGFR kinase domain crystal structures, H773 bonds to the backbone carbonyl oxygen of V851. Mutation of histidine to leucine here may disrupt the local conformation of this loop and influence the catalytic cleft. The other mutations that occur proximal to the kinase catalytic cleft, M793T and T725S, are also close to the adenosine-binding region, with M793T occurring in the kinase hinge segment and T725S in the glycine-rich nucleotide-binding loop. The recent study of Yun et al. (26) illustrates the effects of EGFR point mutations on inhibitor and ATP binding; it is possible that, similar to the Yun study, alterations in the relative kinetics for ATP and CL-387,785 could also play a role in resistance. The transmembrane helix mutations G649R, L655H, L656S, and L658P are intriguing. Previous work has shown that the transmembrane region of EGFR self-associates in cell membranes (31) and that disulfide-induced helix rotation can induce kinase activity (32). Helix rotation was also seen on binding of ATP-competitive inhibitors to the cytoplasmic kinase domain of the protein (32). The discovery of these resistance mutations supports the role of the transmembrane helix in EGFR activation and raises the possibility that a distortion in the interface can interfere with kinase inhibition by certain ATP-competitive inhibitors. The mechanism by which this occurs will need to be further investigated. Interestingly, the originally described oncogenic rat ErbB2 mutation V664E (33) seems to be similar to these transmembrane helix mutations.

It is not clear how the four extracellular domain IV mutations cause resistance to CL-387,785, although expression levels may play a role. Of note, several of these were found as part of double mutant clones, potentially suggesting that some of these might be "carrier" mutations without functional relevance. The EGFR expression level of two of the mutants (Y626H and E545G) was examined and indeed was as high as in nonmutant, high-EGFR colonies (data not shown), suggesting that these mutations might be "silent" and altered expression levels might explain resistance. Whether these mutations affect EGFR expression per se is not yet clear. Irreversible inhibitors covalently bind to C797 of the protein through their Michael acceptor functional group (18, 19, 21). In our studies, this mutation leads to relatively low-level resistance,
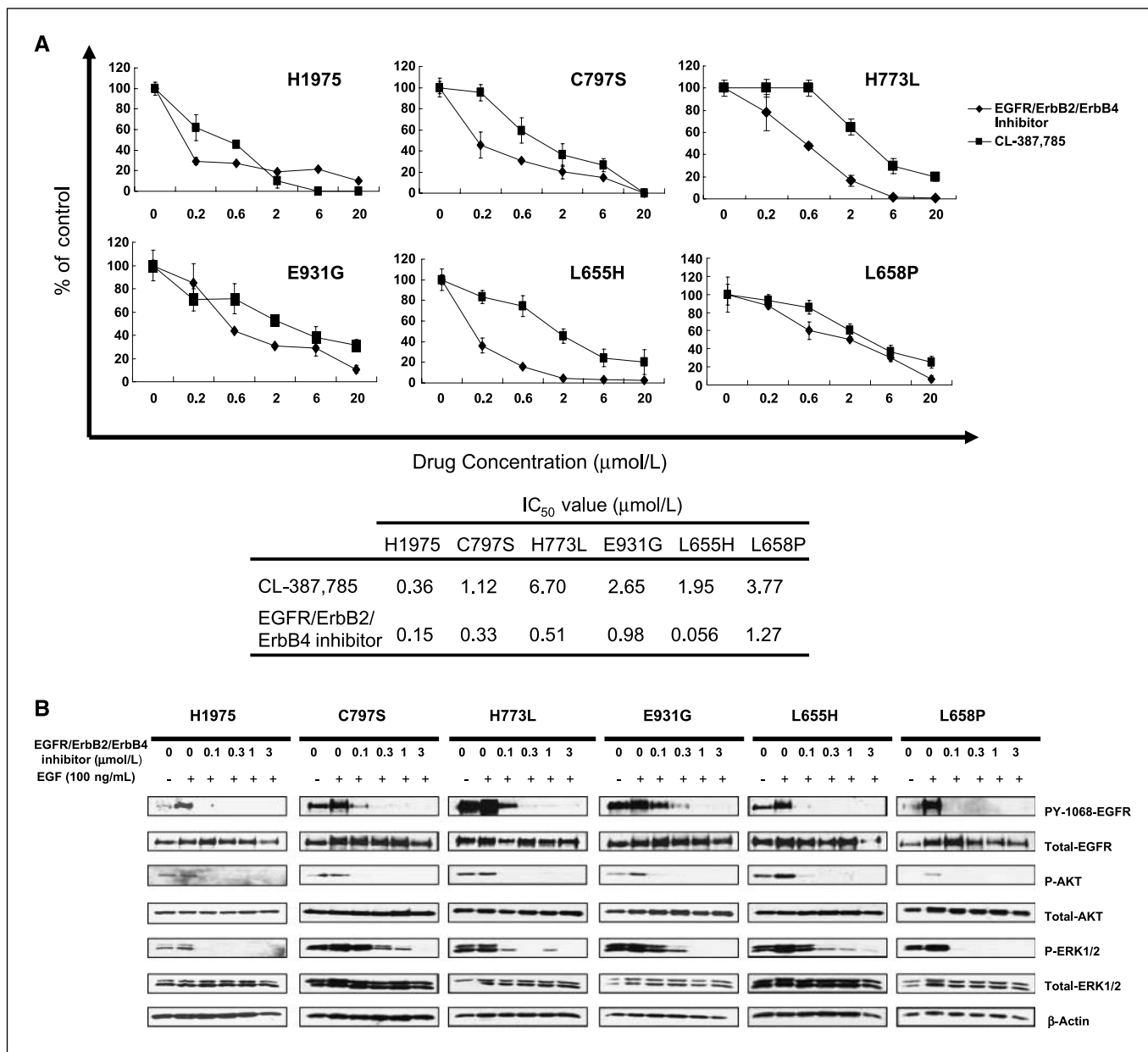
Figure 4. *A,* cellular proliferation of H1975 and mutant H1975 clones at different concentrations of the EGFR/ErbB2/ErbB4 inhibitor and CL-387,785 as determined by the MTS assay. The percentage of cell viability is shown relative to untreated controls. IC_{50} shown in the table was determined from these dose-response curves. *B,* signaling inhibition by EGFR/ErbB2/ErbB4 inhibitor. Cells were incubated in the presence of EGFR/ErbB2/ErbB4 inhibitor at the indicated concentrations for 3 h before stimulation with 100 ng/mL EGF for 15 min. Cell lysates were subjected to SDS-PAGE. Blots were probed for phospho- and total EGFR, AKT, and ERK. β-Actin served as control.

potentially explaining why this mutant was not recovered. In non–small cell lung cancer cells, EGFR mutations are often linked with amplification of the *EGFR* gene. It currently remains unknown whether EGFR amplification leads to resistance against EGFR inhibitors; nonetheless, this mechanism is suggested by our finding that CL-387,785–resistant, transfected H1975 cells without a detectable mutation consistently express EGFR at a higher level as compared with their mutant counterparts or parental H1975 cells. This suggests that similar resistance mechanisms also exist *in vivo* in EGFR-mutant non–small cell lung cancer. In the study of Balak et al. (29), one patient was indeed identified with a significant increase in *EGFR* gene copy number after EGFR tyrosine kinase inhibitor therapy. Whether the mutations identified in our study

lead to functional resistance against other irreversible EGFR inhibitors, such as HKI-272 and EKB-569, will need to be defined individually. At the same time, we believe our model should provide a fair sample of potential resistance mechanisms to be encountered and should also be readily applicable for future studies of EGFR inhibitors. Of note is that our model system focuses on reactivation of EGFR signaling as the mechanism of resistance and therefore is not expected to identify alternative mechanisms, such as the recently described MET amplification (34).

Our studies suggest that tertiary resistance against such inhibitors can be overcome by alternative EGFR inhibitors. Here we used an irreversible pyrido(3,4)-pyrimidine pan-ErbB inhibitor that has nanomolar potency against EGFR, ErbB2, and ErbB4. This
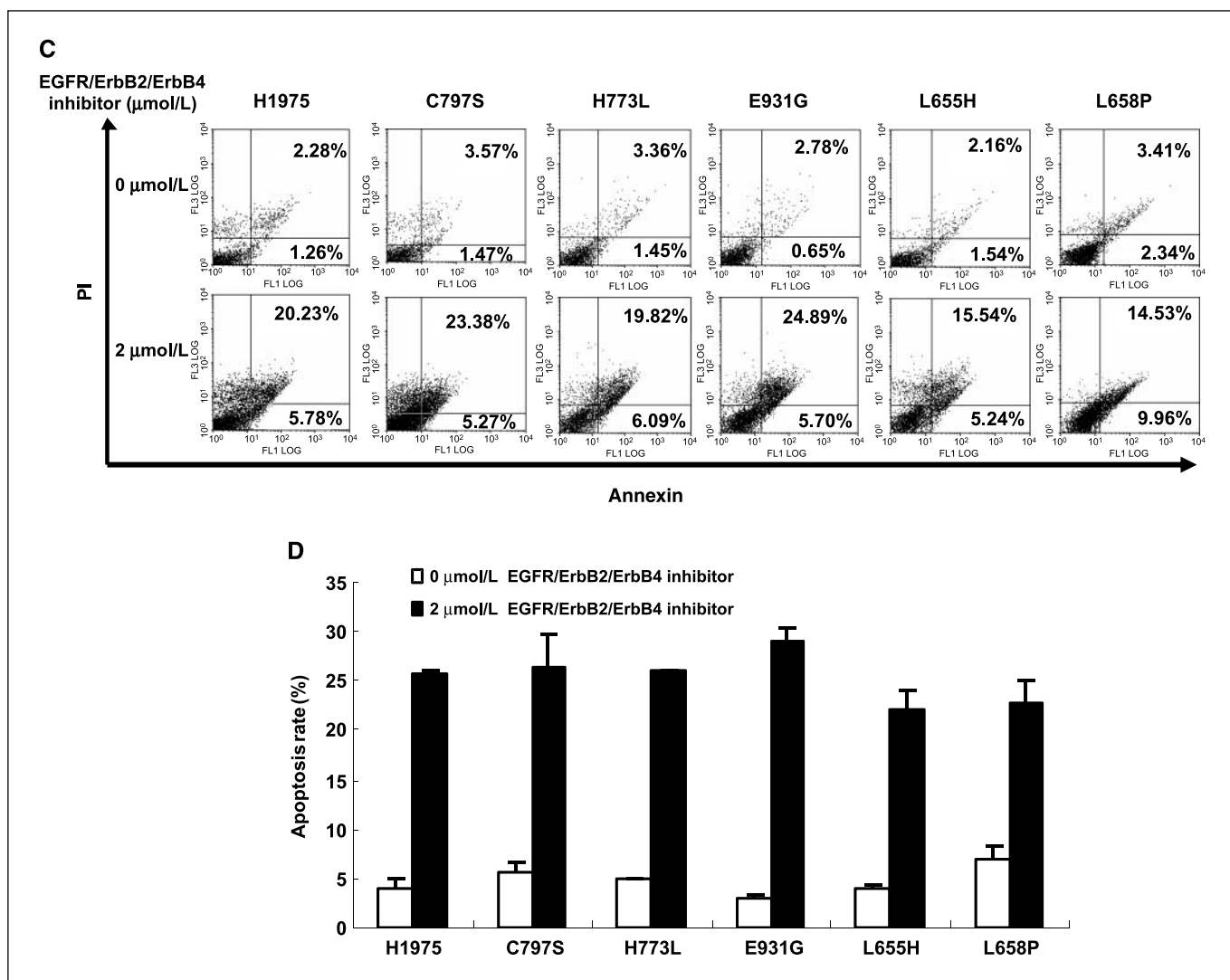
Figure 4 *Continued. C,* EGFR/ErbB2/ErbB4 inhibitor induces apoptosis in parental and mutant H1975 cells. Representative Annexin V/propidium iodide flow cytometry histograms; the numbers represent percent cells in the appropriate quadrant. *D,* quantification of apoptosis.

compound has previously showed great selectivity for EGFR family members over other receptors (e.g., platelet-derived growth factor, fibroblast growth factor, and insulin receptors; ref. 35). This drug showed high-level efficacy against L655H and was only slightly less effective against the C797S and H773L mutants. L658P and E931G cells were more resistant to this compound but the concentrations required to overcome resistance still suggest clinical usefulness. Whether its differential effect is due its higher potency overall or is dependent on its slight structural difference from CL-387,785 will need to be further investigated. This inhibitor, similar to CL-387,785 and other irreversible ErbB inhibitors, is thought to covalently bind to C797 of EGFR. However, the mechanism by which this inhibitor is able to sustain efficacy against the C797S mutation is unclear and may suggest that kinase inhibition does not depend on covalent binding. Clearly, further studies and crystallographic analysis are required and may provide insights such as the Cl-D855 halogen bond seen for gefitinib bound to L858R mutant EGFR (26). The EGFR inhibitor used in our study is multitargeted and blocks the activity of both ErbB2 and ErbB4. Our interpretation of EGFR blockade as its main mechanism of inhibition is supported by our use of the dual EGFR/ErbB2 inhibitor GW583340 that showed no efficacy and signaling studies showing blockade of EGFR activation by this compound on EGF stimulation.

We previously showed that cyclin D1 and downstream regulation of E2F activation are a critical downstream pathway in oncogenic EGFR signaling, suggestive of the therapeutic potential of the cyclin D/Cdk axis (28). In our current studies, we used a selective ATP-competitive Cdk inhibitor (36). This compound in our studies led to S-phase depletion and inhibition of phosphorylation at Cdk phosphorylation sites of Rb in both wild-type H1975 cells and all EGFR-resistant mutant cells tested, consistent with Cdk inhibition. Our current studies further corroborate the importance of the cyclin D/Cdk axis and suggest potential therapeutic benefit in patients with EGFR-mutant non–small cell lung cancer. It will be important to identify whether more potent inhibitors, such as the EGFR inhibitor used in our current studies or combinations of inhibitors (e.g., combined EGFR plus Cdk4 inhibitors), might synergize and thereby prevent or delay the emergence of resistance. Our *in vitro* model system should allow the testing of these concepts.
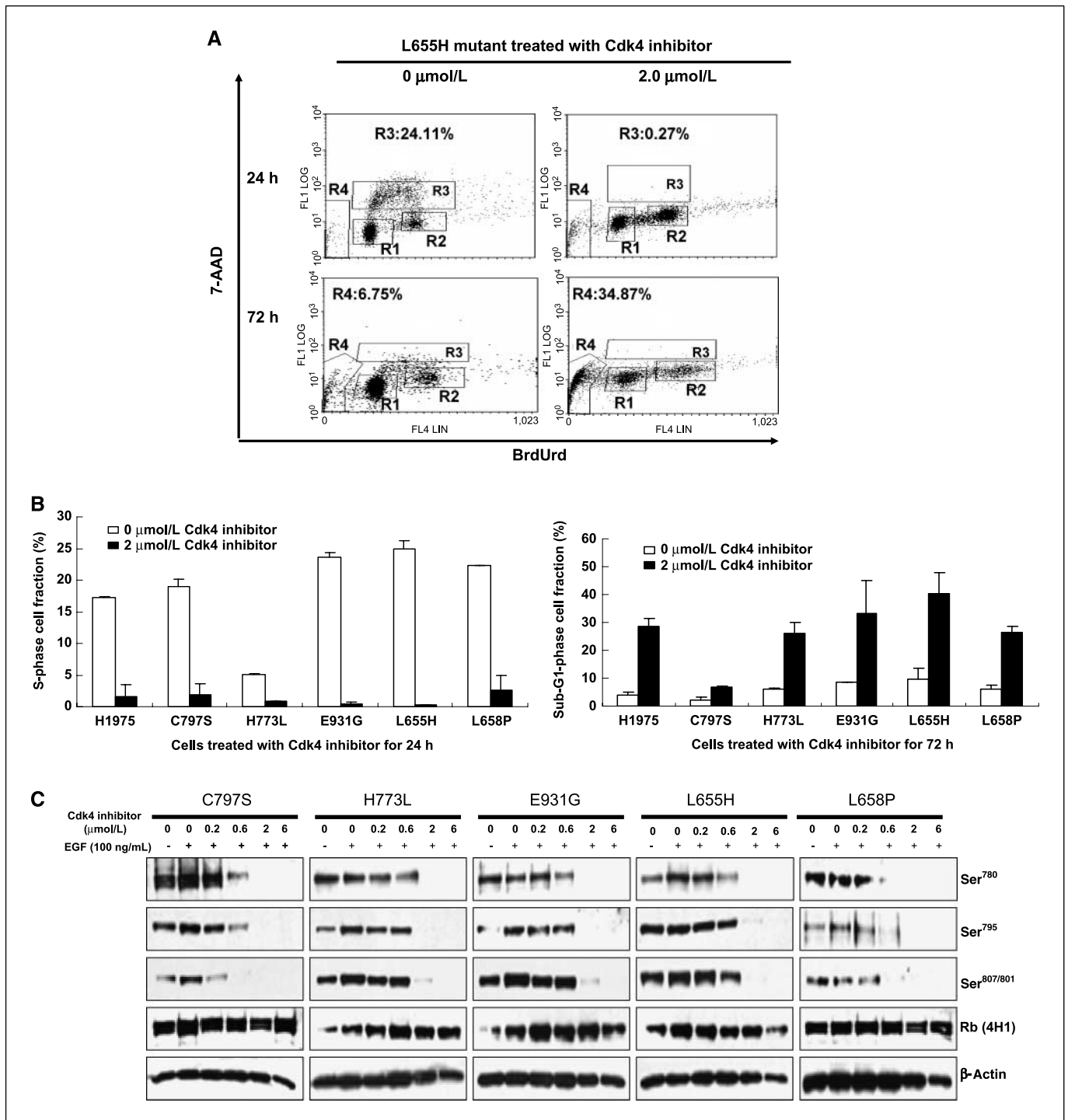
Figure 5. *A,* cells were treated with 2 μmol/L of Cdk4 inhibitor for 24 h. Untreated and treated cells were pulse labeled for 45 min with BrdUrd. Cells were stained with BrdUrd-FITC, counterstained with 7-amino-actinomycin D (*7-AAD*), and analyzed by flow cytometry. *R1,* cells in G$_1$; *R2,* cells in G$_2$-M; *R3,* cells in S phase; *R4,* sub-G$_1$ cells. *B,* percentage of cells in S and sub-G$_1$ phases of the cell cycle after treatment with Cdk4 inhibitor for 24 and 72 h, respectively. *C,* Cdk4 inhibitor treatment leads to hypophosphorylation of Rb. Cells were incubated with Cdk4 inhibitor for 24 h. Protein extracts were analyzed by immunoblotting with phospho-Rb and total Rb specific antibodies. β-Actin was used as control.

Acknowledgments

References

1. Shepherd FA, Rodrigues PJ, Ciuleanu T, et al. Erlotinib in previously treated non-small-cell lung cancer. N Engl J Med 2005;353:123–32.

2. Paez JG, Janne PA, Lee JC, et al. EGFR mutations in lung cancer: correlation with clinical response to gefitinib therapy. Science 2004;304:1497–500.

3. Lynch TJ, Bell DW, Sordella R, et al. Activating mutations in the epidermal growth factor receptor underlying responsiveness of non-small-cell lung cancer to gefitinib. N Engl J Med 2004;350:2129–39.

4. Pao W, Miller V, Zakowski M, et al. EGF receptor gene mutations are common in lung cancers from "never smokers" and are associated with sensitivity of tumors to gefitinib and erlotinib. Proc Natl Acad Sci U S A 2004; 101:13306–11.

5. Jackman DM, Yeap BY, Sequist LV, et al. Exon 19 deletion mutations of epidermal growth factor receptor are associated with prolonged survival in non-small cell lung cancer patients treated with gefitinib or erlotinib. Clin Cancer Res 2006;12:3908–14.

6. Inoue A, Suzuki T, Fukuhara T, et al. Prospective phase II study of gefitinib for chemotherapy-naive patients with advanced non-small-cell lung cancer with epidermal growth factor receptor gene mutations. J Clin Oncol 2006;24:3340–6.

7. Yoshida K, Yatabe Y, Park JY, et al. Prospective validation for prediction of gefitinib sensitivity by epidermal growth factor receptor gene mutation in patients with non-small cell lung cancer. J Thorac Oncol 2007;2:22–8.

8. Rosell R, Taron M, Sanchez JJ, Paz-Ares L. Setting the benchmark for tailoring treatment with EGFR tyrosine kinase inhibitors. Future Oncol 2007;3:277–83.

9. Kobayashi S, Boggon TJ, Dayaram T, et al. EGFR mutation and resistance of non-small-cell lung cancer to gefitinib. N Engl J Med 2005;352:786–92.

10. Pao W, Miller VA, Politi KA, et al. Acquired resistance of lung adenocarcinomas to gefitinib or erlotinib is associated with a second mutation in the EGFR kinase domain. PLoS Med 2005;2:e73.

11. Kwak EL, Sordella R, Bell DW, et al. Irreversible inhibitors of the EGF receptor may circumvent acquired resistance to gefitinib. Proc Natl Acad Sci U S A 2005; 102:7665–70.

12. Kobayashi S, Ji H, Yuza Y, et al. An alternative inhibitor overcomes resistance caused by a mutation of the epidermal growth factor receptor. Cancer Res 2005; 65:7096–101.

13. Carter TA, Wodicka LM, Shah NP, et al. Inhibition of drug-resistant mutants of ABL, KIT, and EGF receptor kinases. Proc Natl Acad Sci U S A 2005;102:11011–6.

14. Yoshimura N, Kudoh S, Kimura T, et al. EKB-569, a new irreversible epidermal growth factor receptor tyrosine kinase inhibitor, with clinical activity in patients with non-small cell lung cancer with acquired resistance to gefitinib. Lung Cancer 2006;51:363–8.

15. Shah NP, Nicoll JM, Nagar B, et al. Multiple BCR-ABL kinase domain mutations confer polyclonal resistance to the tyrosine kinase inhibitor imatinib (STI571) in chronic phase and blast crisis chronic myeloid leukemia. Cancer Cell 2002;2:117–25.

16. Wardelmann E, Merkelbach-Bruse S, Pauls K, et al. Polyclonal evolution of multiple secondary KIT mutations in gastrointestinal stromal tumors under treatment with imatinib mesylate. Clin Cancer Res 2006;12:1743–9.

17. Rice GC, Goeddel DV, Cachianes G, et al. Random PCR mutagenesis screening of secreted proteins by direct expression in mammalian cells. Proc Natl Acad Sci U S A 1992;89:5467–71.

18. Rabindran SK, Discafani CM, Rosfjord EC, et al. Antitumor activity of HKI-272, an orally active, irreversible inhibitor of the HER-2 tyrosine kinase. Cancer Res 2004;64:3958–65.

19. Discafani CM, Carroll ML, Floyd MB, Jr., et al. Irreversible inhibition of epidermal growth factor receptor tyrosine kinase with in vivo activity by N-[4-[(3-bromophenyl)amino]-6-quinazolinyl]-2-butynamide (CL-387,785). Biochem Pharmacol 1999;57:917–25.

20. Ji H, Zhao X, Yuza Y, et al. Epidermal growth factor receptor variant III mutations in lung tumorigenesis and sensitivity to tyrosine kinase inhibitors. Proc Natl Acad Sci U S A 2006;103:7817–22.

21. Fry DW, Bridges AJ, Denny WA, et al. Specific, irreversible inactivation of the epidermal growth factor receptor and erbB2, by a new class of tyrosine kinase inhibitor. Proc Natl Acad Sci U S A 1998;95:12022–7.

22. Stamos J, Sliwkowski MX, Eigenbrot C. Structure of the epidermal growth factor receptor kinase domain alone and in complex with a 4-anilinoquinazoline inhibitor. J Biol Chem 2002;277:46265–72.

23. Wood ER, Truesdale AT, McDonald OB, et al. A unique structure for epidermal growth factor receptor bound to GW572016 (Lapatinib): relationships among protein conformation, inhibitor off-rate, and receptor activity in tumor cells. Cancer Res 2004;64:6652–9.

24. Zhang X, Gureasko J, Shen K, Cole PA, Kuriyan J. An allosteric mechanism for activation of the kinase domain of epidermal growth factor receptor. Cell 2006; 125:1137–49.

25. Jones TA, Zou JY, Cowan SW, Kjeldgaard M. Improved methods for building protein models in electron density maps and the location of errors in these models. Acta Crystallogr A 1991;47:110–9.

26. Yun CH, Boggon TJ, Li Y, et al. Structures of lung cancer-derived EGFR mutants and inhibitor complexes: mechanism of activation and insights into differential inhibitor sensitivity. Cancer Cell 2007;11:217–27.

27. Blair JA, Rauh D, Kung C, et al. Structure-guided development of affinity probes for tyrosine kinases using chemical genetics. Nat Chem Biol 2007;3:229–38.

28. Kobayashi S, Shimamura T, Monti S, et al. Transcriptional profiling identifies cyclin D1 as a critical downstream effector of mutant epidermal growth factor receptor signaling. Cancer Res 2006;66:11389–98.

29. Balak MN, Gong Y, Riely GJ, et al. Novel D761Y and common secondary T790M mutations in epidermal growth factor receptor-mutant lung adenocarcinomas with acquired resistance to kinase inhibitors. Clin Cancer Res 2006;12:6494–501.

30. Debiec-Rychter M, Cools J, Dumez H, et al. Mechanisms of resistance to imatinib mesylate in gastrointestinal stromal tumors and activity of the PKC412 inhibitor against imatinib-resistant mutants. Gastroenterology 2005;128:270–9.

31. Mendrola JM, Berger MB, King MC, Lemmon MA. The single transmembrane domains of ErbB receptors self-associate in cell membranes. J Biol Chem 2002;277: 4704–12.

32. Moriki T, Maruyama H, Maruyama IN. Activation of preformed EGF receptor dimers by ligand-induced rotation of the transmembrane domain. J Mol Biol 2001;311:1011–26.

33. Bargmann CI, Hung MC, Weinberg RA. Multiple independent activations of the neu oncogene by a point mutation altering the transmembrane domain of p185. Cell 1986;45:649–57.

34. Engelman JA, Zejnullahu K, Mitsudomi T, et al. MET amplification leads to gefitinib resistance in lung cancer by activating ERBB3 signaling. Science 2007;316: 1039–43.

35. Klutchko SR, Zhou H, Winters RT, et al. Tyrosine kinase inhibitors. 19. 6-Alkynamides of 4-anilinoquinazolines and 4-anilinopyrido[3,4-d]pyrimidines as irreversible inhibitors of the erbB family of tyrosine kinase receptors. J Med Chem 2006;49:1475–85.

36. Zhu G, Conner SE, Zhou X, et al. Synthesis, structure-activity relationship, and biological studies of indolocarbazoles as potent cyclin D1-4 inhibitors. J Med Chem 2003;46:2027–30.